

# Fatigue Lifetime Estimation of Structures Subjected to Dynamic Loading

D. De Vis,\* R. Snoeys,† and P. Sas‡  
*Katholieke Universiteit Leuven, Heverlee, Belgium*

Because fatigue is a typical dynamic phenomenon, a procedure is developed to estimate the lifetime of a structure, based on its dynamic characteristics. By means of modal analysis, a structure can be described by its modal parameters: mode shapes, natural frequencies, and damping values. Using a finite-element model, the modal stress-strain distribution of part of or an entire structure can be calculated. When the applied dynamic forces are known, combination of the modal strains yields the strain response of the structure. A stress-strain simulation controlled by Neuber's rule accounts for stress concentrations. A counting algorithm based on closed hysteresis loops divides the stress-strain history into single reversals. An appropriate damage rule is used to find the damage of one loading sequence. Finally, the lifetime is found from the number of loading sequences that can be applied to satisfy the failure criterion.

## Introduction

MANY machines and structures fail as a result of metal fatigue. Fatigue is one of the most prevalent and difficult failure modes in fatigue design. This difficulty and uncertainty results in part because commonly used methods of analyzing fatigue are inaccurate and inadequate. Classical approaches are based on static stresses and strains. Fatigue problems, however, are caused by dynamic loading. The amplitude of these dynamic deformations is dominated by damping, while static deformations are controlled only by the structural stiffness. Particularly for lightly damped structures, the dynamic stiffness can be much smaller than the static stiffness. A factor of 50 to 100 is not unusual.<sup>1</sup> Therefore, it is important to include the dynamic behavior in lifetime calculations.

The dynamic behavior of a structure can be determined using experimental modal analysis. In the present paper, we will explain how the strain response of this structure can be computed when the applied forces are known. Since fatigue is a localized phenomenon, attention is focused on the regions of a component where failure is likely to initiate. In order to account for local stress concentrations, a link is made between nominal and local strain sequences. A lifetime prediction procedure based on a stress-strain simulation, using the cyclic stress-strain curve, and the fatigue characteristics of the material yields the lifetime of the structure. If the calculated lifetime is not acceptable, different redesign options can be taken: material choice, changing external dynamic loads, or modifying the dynamic behavior. Depending on the boundary conditions of the design, some of these options may require more effort than others. For example, sensitivity analysis and modal synthesis techniques<sup>2</sup> will provide the optimal structural modifications and the new dynamic characteristics. A new lifetime calculation can then be started without further experimental testing or prototype construction. (See Fig. 1.<sup>3</sup>)

Fatigue and reliability tests of components, subassemblies, and complete structures are, and will continue to be, necessary, in order to confirm experimentally that a given design is adequate. Whenever possible, the intent should be

to use these tests for design validation and not for design development. In particular, the very expensive practice of iterative testing, in which a component is designed and tested, and redesigned and retested, until an adequate solution is obtained, can frequently be avoided if more appropriate analytical techniques are used.

## Modal Description of the Structural Dynamics

The relation between the response of a linear system and the applied dynamic loads can be written in terms of the following frequency-response function matrix<sup>4</sup>:

$$\{X(j\omega)\} = [H(j\omega)] \{F(j\omega)\} \quad (1)$$

where  $\{X(j\omega)\}$  is the vector containing the Fourier transform of responses,  $\{F(j\omega)\}$  the vector containing the Fourier transform of applied forces, and  $[H(j\omega)]$  the matrix of measured frequency-response functions. In general, only a few rows or columns of the matrix  $H$  are measured, so that  $H$  is not square. By means of curve-fitting algorithms, we identify the different modes by their modal parameters: mode shape, natural frequency, and damping value. Equation (1) is now rewritten in terms of its modal parameters:

$$\{X(j\omega)\} = \left[ \sum_{k=1}^N \left( \frac{[U_{Ijk} + jV_{Ijk}]}{-u_k + j(\omega - v_k)} + \frac{[U_{Ijk} - jV_{Ijk}]}{-u_k + j(\omega + v_k)} \right) \right] \{F(j\omega)\} \quad (2)$$

where

$I, J$	= response and excitation points, respectively
$k$	= mode number
$N$	= number of modes
$\{X\}, \{F\}$	= response and force vectors, respectively
$U_{Ijk}$	= real part of modal displacement for mode $k$ of point $I$ for excitation in point $J$
$V_{Ijk}$	= imaginary part of modal displacement for mode $k$ of point $I$ for excitation in point $J$
$v_k$	= damped natural frequency for mode $k$
$u_k$	= damping value for mode $k$ .

As mentioned previously, only a limited number of input points are used during the analysis. Under normal working

Received April 4, 1985; revision received Sept. 27, 1985. Copyright © American Institute of Aeronautics and Astronautics, Inc., 1985. All rights reserved.

\*Research Fellow, Department of Mechanical Engineering; currently at Leuven Measurement and Systems.

†Professor, Department of Mechanical Engineering.

‡Research Associate, Belgian Funds of Scientific Research (NFWO).

conditions, the structure will not necessarily be loaded at these points. Therefore, we must calculate the modal displacement for excitation in the loaded points, so that the frequency-response matrix elements to be multiplied by a nonzero force are known. This can easily be done when the following conditions are met: 1) the direct frequency-response functions are known, and 2) points that are loaded under normal operation are contained in the set of measurement points.

When  $J$  is the excitation point, the modal displacement of point  $I$  for the mode  $k$  can be written as

$$U_{Ijk} + jV_{Ijk}$$

The modal displacement of point  $I$  for mode  $k$  and input point  $L$  can then be calculated, using the eigenvector expression for the modal displacements:

$$\begin{aligned} U_{Ijk} + jV_{Ijk} &= \frac{\Psi_{Ik} \Psi_{Lk}}{a_k} = \frac{\Psi_{Ik} \Psi_{Jk} \Psi_{Lk} \Psi_{Jk}}{a_k \Psi_{Jk} \Psi_{Jk}} \\ &= \frac{(U_{Ijk} + jV_{Ijk})(U_{Ljk} + jV_{Ljk})}{U_{Jjk} + jV_{Jjk}} \end{aligned} \quad (3)$$

where  $a_k$  can be chosen arbitrarily since eigenvectors are only defined as a direction in the state space and have no absolute magnitude. Using Eq. (3), the transfer function matrix can be made square. Dynamic loads can then be applied to all measurement points on the structure and the response vector in the frequency domain can be computed. The response in the time domain is found by the inverse Fourier transform of Eq. (2). The theory reviewed above is valid for whatever physical quantity (displacement, speeds, accelerations, strains, etc.) are measured, as long as the response is related to the input on a linear basis. Since it is a rather difficult task to measure the strain history directly, an alternative computation method was developed.

### Modal Strains and Strain History

The knowledge of the strain history at the critical points is essential for the lifetime estimation of structures subjected to dynamic loading. This section describes a procedure to generate these strain histories, starting from a known dynamic force, and the modal strains, eigenvectors, and measured mode shapes. Eigenvectors only define a direction in the state space and have no amplitude. Experimental mode shapes have a physical meaning and amplitude; for example, for a force input of  $xN$  in point  $A$  we obtain an acceleration of  $y \text{ m/s}^2$  in point  $B$ .

Modal strains are defined as the strains measured at the different response points on the structure, when the structure is excited at resonance frequency. As mentioned previously, carrying out a modal analysis with strain gages is a rather time-consuming task. Therefore, we preferred to calculate rather than measure the modal strains. This allows a classical modal analysis, using input forces and response accelerations. The modal accelerations can be scaled to modal deformations through division by the squared resonance pulsation. It is clear that, similar to modal deformations, modal strains will depend on both the input and response points. From the basic assumption of modal analysis there is a linear relationship between input and output. The strain responses to be calculated are linearly related to the applied forces, while, in reality, local plastic yielding often causes nonlinear effects. These nonlinearities will be accounted for in a second step by using a cyclic stress-strain relationship and Neuber's rule, as explained in the next section.

Modal strains can be calculated in different ways. One method consists of postulating an analytical function for the deflections and fitting it to the experimentally determined mode shapes. The modal strains then result directly from the

theory of elasticity. This method was implemented at the Katholieke Universiteit Leuven (K.U.L.) for beam-like structures. The bending modes are approximated by a set of orthogonal polynomials, using a least-squares algorithm. The order of the polynomials is automatically determined by analyzing the least-squares error evolution for increasing order. Second-order derivation and multiplying by the distance to the neutral axis yields the strain. The advantage of this method is speed. On the other hand, for complex structures, it may be rather cumbersome and difficult to find an analytical expression for the mode shape. Another problem is that numerical differentiation is a highly unstable process, therefore, results must be interpreted with care.

A more general approach uses a static finite-element model. Basically, the mode shape is imposed as a static deformation pattern to compute the modal strains. Rotational degrees of freedom remain free.

The approach used at the K.U.L. differs slightly (see Fig. 2); due to the lack of a finite-element program that allows imposing a deformation pattern, a dynamic finite-element model was used to compute the eigenvectors.<sup>5</sup> Once these are known, stress calculations are carried out to find the modal stresses and strains. The analytical eigenvectors are compared to the experimental mode shapes with the modal assurance criterion.<sup>6</sup> The modal scale factor, which expresses

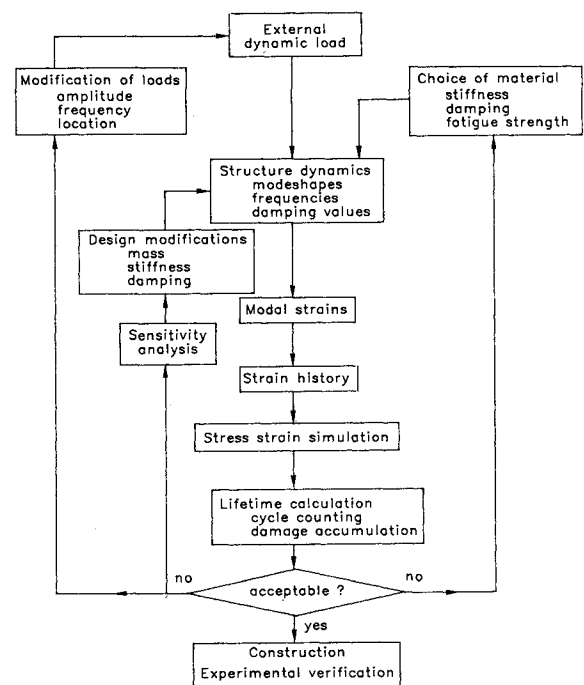


Fig. 1 Flowchart of design against fatigue (Ref. 1).

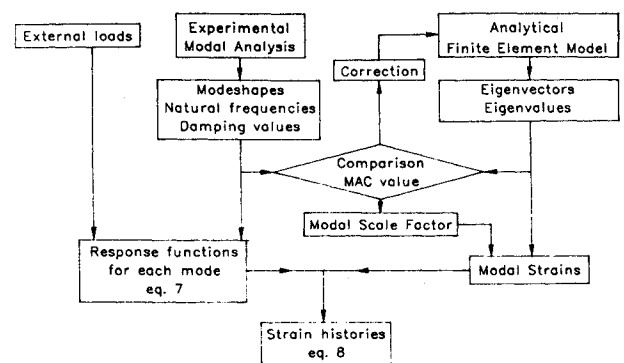


Fig. 2 Flowchart of nominal strain history calculation.

the ratio between the experimental and analytical amplitudes of the mode shapes, is used to scale the calculated strains.

Another possible approach calculates the inertia forces at the resonance frequency. Applying those to a static model should yield a deflection very close to the mode shape, so that modal strains can be computed.

All of the calculation procedures mentioned above have the common advantage of reducing measurement errors by smoothing the mode shape in one way or another. Moreover, it becomes possible to estimate modal strains in points that were not measured originally.

Once the modal strains are known, it is possible to rewrite Eq. (2) in terms of modal strains.  $\{X\}$  then defines the strain response in the frequency domain. The inverse Fourier transform of Eq. (2) yields the following strain histories<sup>7</sup>:

$$\{x(t)\} = \int_0^t \sum_{k=1}^N \{ [S_{Ijk} + jT_{Ijk}] \exp[(u_k + jv_k)r] + [S_{Ijk} - jT_{Ijk}] \exp[(u_k - jv_k)r] \} \{f(t-r)\} dr \quad (4)$$

with  $S_{Ijk} + jT_{Ijk}$  the modal strain in point I, input point J for mode  $k$ .

In order to eliminate the repeated calculation of the modal strains and exponentials, Eq. (4) can be rewritten as

$$\{x(t)\} = 2 \sum_{k=1}^N [S_{Ijk}] \int_0^t e^{u_k} (\cos v_k r) \{f(t-r)\} dr + 2 \sum_{k=1}^N [jT_{Ijk}] \int_0^t e^{u_k} (j \sin v_k r) \{f(t-r)\} dr \quad (5)$$

If we define the vector of response functions for mode  $k$  as

$$\{R_k(t)\} = \int_0^t \exp[(u_k + jv_k)r] \{f(t-r)\} dr \quad (6)$$

then Eq. (5) can be written as

$$\{x(t)\} = 2 \sum_{k=1}^N ([S_{Ijk}] \operatorname{Re}\{R_k(t)\} - [T_{Ijk}] \operatorname{Im}\{R_k(t)\}) \quad (7)$$

Equations (6) and (7) allow us to compute the strain history in each measured point, or in intermediate points, with a certain precaution. This computation algorithm is much faster than the straightforward approach of computing the responses in the frequency domain explicitly and performing an inverse fast Fourier transform (FFT) to obtain the time-domain histories. Figure 3 shows the calculated strain response of a point on a T plate, due to a hammer impact.

The strain histories are linear combinations of the modal strains, with the response functions as weighting functions, as long as no plastic yielding occurs. Figure 3 clearly shows the different modes in the time response. It will be clear that, due to the method used to obtain the modal strains, the resulting strain histories are so-called nominal strains. It was also assumed that the deformation remained completely elastic. At this point no information is available relative to the local high strains that may occur at points of stress concentration. Since cracks will originate at points of stress concentration, it is of major importance to evaluate those local strain histories. Local strains could be evaluated using a finite-element model with many nodal points in the critical areas, in combination with a curve expressing the elastic-plastic stress-strain relationship during cyclic loading. These sophisticated models require a sizable amount of computation time, as well as a powerful computer. The next section

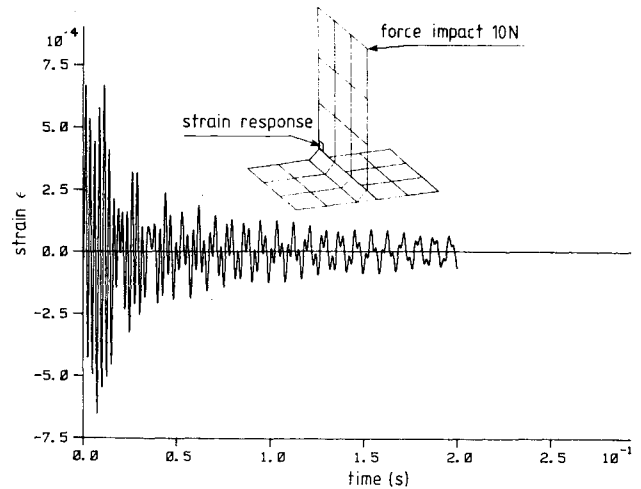


Fig. 3 Calculated strain response on a T plate.

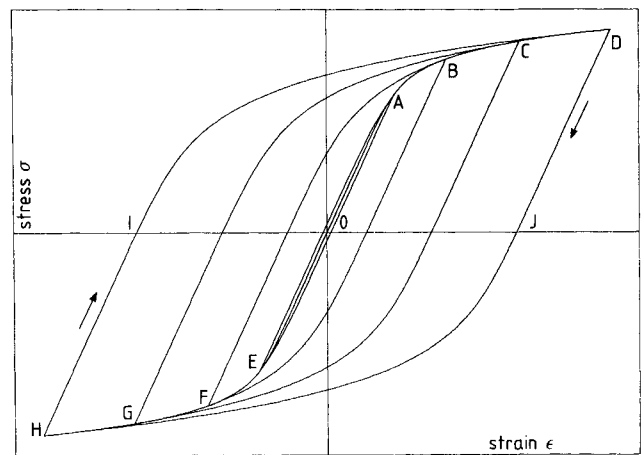


Fig. 4 Cyclic stress-strain curve determined from a set of stable hysteresis loops.

describes a cheaper link between the nominal deformation and the local strains and stresses.

### Stress-Strain Simulation

Fatigue problems in a dynamically loaded mechanical structure arise at stress concentrations. The gross deflections of the structure are related to the applied loads in a linear elastic manner. In other words, there is no general yielding, but plastic strains may occur at the critical locations. Furthermore, at those points of stress or strain concentration, the stress-strain path will not follow the monotonic stress-strain curve but will describe closed hysteresis loops. In this section, we will describe how the local stress-strain histories can be derived from the nominal strain sequence using the cyclic stress-strain curve and Neuber's rule.

During a constant-amplitude, controlled strain test, after the initial rapid hardening or softening is complete, a stable stress-strain hysteresis loop is formed. If loops from tests at several different strain levels are plotted on the same axes, the cyclic stress-strain curve is defined by the locus of the loop tips (Fig. 4). If a log-log plot is made of stress vs plastic strain, a straight line results, implying a mathematical relationship for the total strain<sup>8</sup>:

$$\epsilon_a = (\sigma_a/E) + (\sigma_a/A)^{1/s} \quad (8)$$

where  $A$  and  $s$  are material properties.

During cyclic loading the material does not follow the cyclic stress-strain curve as a loading path in the same sense as a monotonic stress-strain curve. Rather, hysteresis loop curves such as DJHID in Fig. 4 are formed. When hysteresis loops are drawn on shifted axes, so that their compressive tips coincide, the tensile tips of the loops must coincide with the cyclic stress-strain curve expanded by a factor of 2. Thus, a stable hysteresis loop trace for a given metal follows a curve which may be mathematically described by expanding the cyclic stress-strain curve by a factor of 2 and shifting its origin. For hysteresis loop curves during increasing strain, the following equation applies<sup>8</sup>:

$$\frac{\epsilon - \epsilon_r}{2} = \frac{\sigma - \sigma_r}{2E} + \left( \frac{\sigma - \sigma_r}{2A} \right)^{1/s} \quad (9)$$

where  $(\sigma, \epsilon)$  are instantaneous stress and strain, and  $(\sigma_r, \epsilon_r)$  are the coordinates of the previous point of strain reversal. By appropriate sign changes, a similar equation is obtained for hysteresis loop curves during decreasing strain:

$$\frac{\epsilon_r - \epsilon}{2} = \frac{\sigma_r - \sigma}{2E} + \left( \frac{\sigma_r - \sigma}{2A} \right)^{1/s} \quad (10)$$

For an irregular strain history, a set of closed stress-strain hysteresis loops is formed. A closed hysteresis loop may be temporarily interrupted while one or more smaller closed

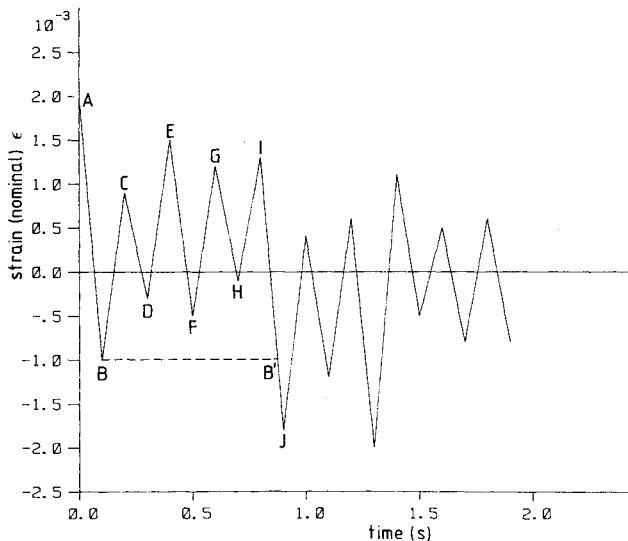


Fig. 5a Nominal strain sequence.

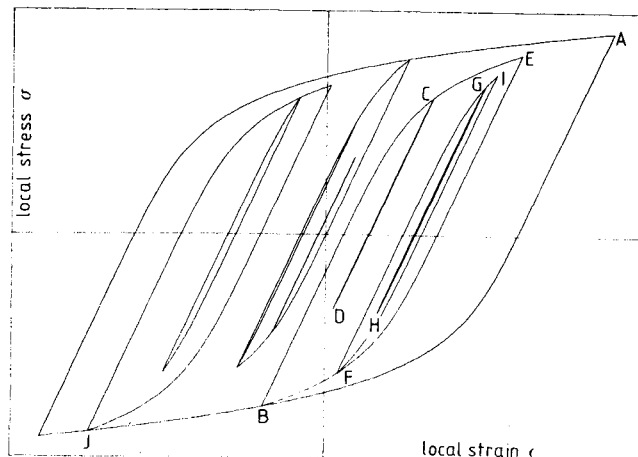


Fig. 5b Local stress-strain evolution.

loops are completed. For example, in Fig. 5b, which is the local stress-strain simulation, corresponding to the nominal strain sequence in Fig. 5a, the loop corresponding to strain excursion B-E is interrupted by smaller loops corresponding to strain excursions C-D and F-I, with the latter being interrupted by an even smaller loop, G-H. This phenomenon is called memory. This memory effect can be characterized in a general manner by two rules: 1) The next time the strain reaches a value at which the straining direction was previously reversed, a hysteresis loop is closed. 2) As soon as a strain excursion forms a closed loop, this excursion does not affect the subsequent behavior; the stress-strain path beyond this point is the same as if the direction of straining had not been reversed.

In the previous paragraphs, a philosophy to calculate the shape of the hysteresis loops was explained. The only missing link is a relationship between the nominal elastic strains and the local (possibly plastic) strains occurring at a stress concentration. This relationship is given by Neuber's rule.<sup>9</sup> He postulated that during local plastic deformation the geometric mean of stress and strain concentration factors ( $k_\sigma$  and  $k_\epsilon$ ) remains equal to the elastic stress concentration factor  $k_t$ :

$$\sqrt{k_\sigma k_\epsilon} = k_t \quad (11)$$

As long as the gross deformation remains elastic, the following form results:

$$\sqrt{\Delta\sigma\Delta\epsilon} = k_t \Delta S \quad (12)$$

where  $\Delta S$  is the nominal stress range, which is equal to the nominal strain range times the elastic modulus  $E$ . The product of local stress ( $\Delta\sigma$ ) and strain ( $\Delta\epsilon$ ) is a constant for a given stress concentration factor ( $k_t$ ) and a known nominal strain variation. In a stress-strain plot, Neuber's rule defines a hyperbola.

A computer program was developed to simulate the local stress-strain path starting from a nominal strain history which was obtained as explained in the preceding sections (see Fig. 6).

Figure 5 has already illustrated the principle of the calculation. In Fig. 5, however, the stress concentration factor was largely exaggerated, so that the different reversals could be

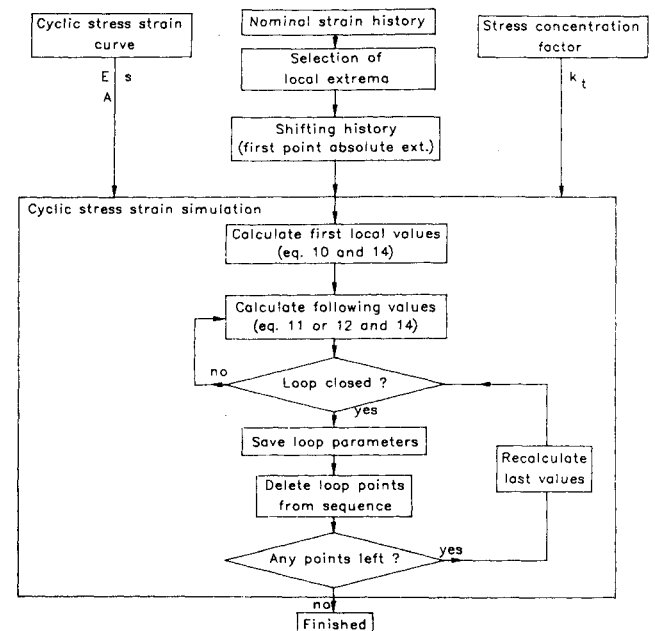


Fig. 6 Local stress-strain simulation and individual cycle definitions.

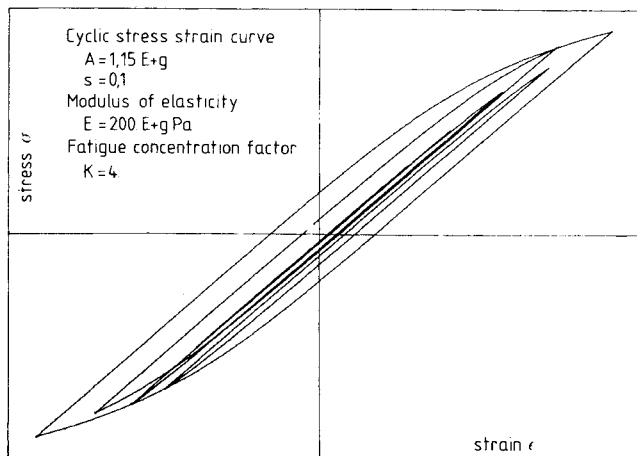


Fig. 7 Local stress and strain, derived from the nominal strain in Fig. 3.

seen as wide hysteresis loops. The strain history of Fig. 3 was analyzed following the same procedure, but with a realistic stress concentration factor. The plot in Fig. 7 shows that only a few, still narrow, loops occur. Most of the reversals remain in the elastic region and coincide in the center of the plot. The software automatically provides these plots during the analysis for visual inspection of the degree of plasticity for the particular location.

This method of separating individual cycles by means of closed hysteresis loops is clearly very similar to the Rainflow counting algorithm. For more details concerning methods of fatigue-life prediction we refer to the literature where excellent reviews of the subject can be found (see Refs. 11-14).

### Damage Calculation and Cumulation

At this stage, a critical strain history was divided into several closed hysteresis loops. Each of the individual hysteresis loops is completely characterized: both the stress and strain amplitude and mean values are known. Due to the memory effect, these loops can be regarded as completely separate events. This allows us to compute the damage of each loop separately. Summing these damages individually yields the total damage due to the analyzed sequence, resulting in the lifetime of the structure in terms of the number of sequences analyzed. This information easily yields the lifetime in physical units, i.e., hours of operation, kilometers driven, etc.

Damage for a single hysteresis loop is estimated by means of a lifetime curve. The analytical representation of this strain-life curve is expressed by the following equation<sup>10</sup>:

$$\frac{\Delta\epsilon}{2} = \frac{\sigma_f'}{E} (2N_f)^b + \epsilon_f' (2N_f)^c \quad (13)$$

where

- $\Delta\epsilon/2$  = strain amplitude
- $E$  = elastic modulus
- $\sigma_f', \epsilon_f'$  = fatigue strength and ductility coefficients, respectively
- $b, c$  = fatigue strength and ductility exponents, respectively
- $N_f$  = reversals to failure

In this representation, the strain-cycling resistance of a material is viewed as the sum of its elastic (governed by strength) and plastic (governed by ductility) strain resistance (Fig. 8). It is completely determined by four additional material constants, which make it possible to set up a

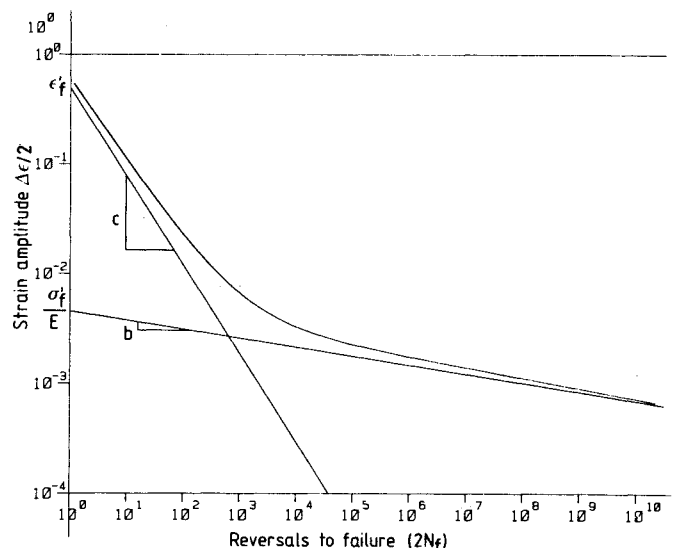


Fig. 8 Lifetime curve.

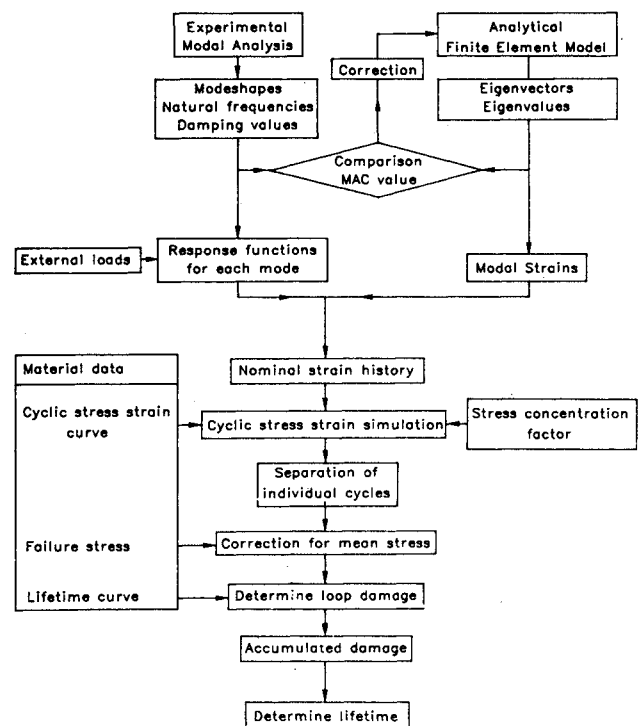


Fig. 9 Lifetime calculation.

material fatigue data base with a very limited amount of numbers.

Material lifetime curves are measured for completely reversed stress or strain cycles. A reversal with a tensile mean stress will open an initial microcrack further than a reversal having the same amplitude, but a zero or compressive mean stress. If the mean stress is tensile, the  $N_f$  value must be decreased to reflect the detrimental effect of a tensile mean stress.

If we use the lifetime curve defined by Eq. (13), we can make a correction in the equation for nonzero mean stresses. Mean stresses are not important when large plastic strains occur because the material accommodates by plastic deformation, transferring its share of the mean load to the surrounding elastic material. This means that only the elastic

portion of Eq. (13) needs to be changed:

$$\frac{\Delta\epsilon}{2} = \frac{(\sigma_f' - \sigma_m)}{E} (2N_f)^b + \epsilon_f' (2N_f)^c \quad (14)$$

The damage for each closed hysteresis loop can then be evaluated. The total damage is given by the linear damage accumulation rule of Palmgren-Miner:

$$D = \sum_i \left( \frac{1}{N_i} \right) \quad (15)$$

The total lifetime expressed as the number of applied histories becomes  $1/D$ .

### Conclusions

The procedure based on experimental modal parameters has the advantage of explicitly accounting for the dynamic stiffness. To perform a modal analysis, it is not necessary to build a complete operational prototype. Only the analyzed substructure should be built with simulated boundary conditions, while for experimentally measuring strain responses the applied loads also must be simulated, or a complete prototype operated. As a consequence, fatigue analysis can be carried out early in the design phase.

Sensitivity analysis of the modal parameters can be of great help when the design of a particular substructure is unacceptable. Using modal synthesis techniques, the effect of some structural modifications on the modal parameters can be predicted. After adequately modifying the finite-element model, a new analysis can be carried out without requiring reconstruction of a prototype. In this way, the iterative testing and redesigning will become largely a numerical process rather than an expensive experiment.

Modal parameters (mode shapes, natural frequencies, and damping values) describe the dynamic behavior of a structure completely. In combination with a finite-element model and the applied forces, the lifetime is estimated using the material fatigue data (Fig. 9). During this analysis it is important to account for stress concentrations. This can be done either by using a detailed finite-element model or by applying Neuber's rule. The amount of material data can be kept very condensed: the modulus of elasticity, the cyclic stress-strain curve (two parameters), and the lifetime curve (four parameters) or a total of only seven material constants. In addition to the modal parameters obtained experimentally on a (substructure of a) prototype a complete geometric description is required to build a finite-element model. The applied forces, as a function of time, should also be known. Information about stress concentrations should be available in terms of a stress concentration factor.

Experimental fatigue and reliability testing will, however, remain necessary. Due to scatter of material properties and some inherent limitations of Neuber's rule, as well as Palmgren-Miner's rule, analytical lifetime calculations remain approximations.

### Acknowledgment

This research was financially supported by the Belgian Institute for Scientific Research in Industry and Agriculture.

### References

- <sup>1</sup>Vandeuren, U., "Identification of Damping in Materials and Structures. Optimization of the Dynamic Behavior of Mechanical Structures," Ph.D. Dissertation, Katholieke Universiteit Leuven, Belgium, 1982.
- <sup>2</sup>Vanhonacker, P., "The Use of Modal Parameters of Mechanical Structures in Sensitivity Analysis, System Synthesis, and System Identification Methods," Ph.D. Dissertation, Katholieke Universiteit Leuven, Belgium 1980.
- <sup>3</sup>Snoey, R. and Van Brussel, H., "Berekenen en Dimensioneren tegen vermoeing," Katholieke Universiteit Leuven, Uitg. Universitas Antwerpen, Standaard boekhandel, Dec. 1984.
- <sup>4</sup>*Proceedings of the Yearly International Seminar on Modal Analysis*, Katholieke Universiteit Leuven, Belgium, 1976-1984.
- <sup>5</sup>Verdonck, E. and Snoey, R., "Life Time Prediction Based on the Combined Use of Finite Element and Modal Analysis Data," *Proceedings of the 8th International Seminar on Modal Analysis*, Katholieke Universiteit Leuven, Belgium, Sept. 1983.
- <sup>6</sup>Allemang, R. J., "Concept and Application of Modal Scale Factor and Modal Assurance Criterion," Ph.D. Dissertation, University of Cincinnati, Ohio, 1980, pp. 141-162.
- <sup>7</sup>Verdonck, E., "Response Calculation of Dynamical Structures," *Proceedings of the 7th International Seminar on Modal Analysis*, Katholieke Universiteit Leuven, Belgium, Sept. 1982.
- <sup>8</sup>Landgraf, R. W. and LaPointe, N. R., "Cyclic Stress-Strain Concepts Applied to Component Fatigue Life Prediction," SAE 740280, 1974.
- <sup>9</sup>Neuber, H., "Theory of Stress Concentration for Shear Strained Prismatical Bodies with Arbitrary Nonlinear Stress Strain Law," *Journal of Applied Mechanics, Transactions of ASME*, Vol. 28, Dec. 1961, pp. 554-550.
- <sup>10</sup>Dilger, T. C., "Developing and Validating a 'User-Oriented' Fatigue Analysis Program," SAE 800686, April 1980.
- <sup>11</sup>Wetzel, R. M., "A Method of Fatigue Damage Analysis," ASME Materials Science Seminar, St. Louis, MO, Oct. 1978.
- <sup>12</sup>Dowling, N. E., "Fatigue Failure Predictions for Complicated Stress-Strain Histories," *Journal of Materials*, Vol. 7, No. 1, 1972, pp. 71-87.
- <sup>13</sup>Mitchell, M. R., "Fundamentals of Modern Fatigue Analysis for Design," *Fatigue and Microstructures*, 1979, pp. 385-437.
- <sup>14</sup>Socie, D. F. and Morrow, J., "Review of Contemporary Approaches to Fatigue Damage Analysis," *Risk and Failure Analysis for Improved Performance and Reliability*, edited by J. Burke and V. Weiss, Plenum Publishing, New York, 1980, Chap. 8, pp. 141-193.